

# Relational color constancy in achromatic and isoluminant images

Sérgio M. C. Nascimento and David H. Foster

*Departamento de Física, Universidade do Minho, 4709 Braga Codex, Portugal, and Visual and Computational Neuroscience Group, Department of Optometry and Neuroscience, University of Manchester Institute of Science and Technology, Manchester M60 1QD, UK*

Received April 28, 1999; revised manuscript received September 27, 1999; accepted October 8, 1999

Relational color constancy, which refers to the constancy of perceived relations between surface colors under changes in illuminant, may be based on the computation of spatial ratios of cone excitations. As this activity need occur only within rather than between cone pathways, relational color constancy might be assumed to be based on relative luminance processing. This hypothesis was tested in a psychophysical experiment in which observers viewed simulated images of Mondrian patterns undergoing colorimetric changes that could be attributed either to an illuminant change or to a nonilluminant change; the images were isoluminant, achromatic, or unmodified. Observers reliably discriminated the two types of changes in all three conditions, implying that relational color constancy is not based on luminance cues alone. A computer simulation showed that in these isoluminant and achromatic images spatial ratios of cone excitations and of combinations of cone excitations were almost invariant under illuminant changes and that discrimination performance could be predicted from deviations in these ratios. © 2000 Optical Society of America [S0740-3232(00)01502-7]

OCIS codes: 330.0330, 330.1720, 330.1690, 330.4060.

## 1. INTRODUCTION

In the physical world, the spectral composition of the light reflected from the surfaces in a scene varies with the incident illumination, for example, with the phase of daylight or as daylight changes to artificial light. Two kinds of colorimetric constancies that might hold under these conditions are color constancy and relational color constancy. Color constancy refers to the invariance of the perceived colors of the surfaces under changes in illuminant. This form of color constancy has often been assumed,<sup>1-5</sup> but, in practice, measurements of observers' ability to make color-constancy judgments show that they have a variable competence.<sup>6-17</sup> In contrast, relational color constancy refers to the invariance of the perceived relations between the colors of the surfaces under changes in illuminant. This constancy might explain the remarkable ability of observers to discriminate reliably and effortlessly between illuminant changes in a scene and changes in the materials making up that scene.<sup>18,19</sup> Relational color constancy is different from color constancy in that it is not assumed that the perceived colors of surfaces remain constant in any given illuminant change. There is, however, a close relationship between the two phenomena (see Ref. 20, Appendix 1).

The coding of the perceived relations between surface colors could be based on the ratios of cone excitations generated in response to light reflected from pairs of surfaces. In general, these spatial ratios of excitations—within the same cone class and across spatially distinct regions—are remarkably stable under large changes in the color temperature of the illuminant (e.g., 2000–100,000 K for a Planckian source) and over a wide range of spectral re-

flectances (the Munsell set).<sup>20</sup> This putative role of spatial cone-excitation ratios in coding perceived color relations is consistent with the results of experiments designed to measure the detectability of deviations in these ratios under illuminant changes.<sup>21</sup> Thus observers were presented with simulations of Mondrian patterns undergoing two kinds of illuminant changes in a two-interval design. In one interval the surfaces underwent a natural illuminant change selected so that spatial cone-excitation ratios were not quite invariant; in the other interval the surfaces underwent the same change, except that the images were corrected so that ratios were preserved exactly. Although the intervals with corrected images corresponded individually to highly improbable natural events, observers systematically misidentified them as containing the illuminant changes.

The fact that discrimination performance can be explained by activity within rather than between cone pathways might suggest that the visual system is concerned only with relative luminance, so that relational color constancy would be little more than a form of lightness constancy; that is, the constancy of perceived achromatic contrast under changes in illumination level.<sup>22-24</sup> To test this hypothesis, the present experiment was undertaken. Simulated images of Mondrian patterns were presented undergoing colorimetric changes that could be attributed either to an illuminant change or to a nonilluminant change. The images were isoluminant, so that there were no luminance cues<sup>25</sup>; achromatic, so that there were no chromatic cues; and, as a control, unmodified, where luminance and chromaticity varied freely. Observers made reliable discriminations between illuminant-

derived and nonilluminant-derived changes with all three types of images, implying that relational color constancy was not based simply on luminance processing.

The achromatic and isoluminant images represent impoverished worlds whose reflectances and illuminants would be very improbable in the natural world. Are, then, spatial ratios of cone excitations still stable under these illuminant-derived changes? To answer this question, simulations of cone activity were computed with these modified images. It was found that spatial ratios of cone excitations and of combinations of cone excitations were almost invariant in these extreme conditions and that discrimination performance could be well predicted from deviations in these ratios.

## 2. PSYCHOPHYSICS

### A. Methods

#### 1. Apparatus

Stimuli were generated by a RGB color-graphics system (Visual Stimulus Generator 2/3, Cambridge Research Systems, Rochester, UK) under the control of a computer and displayed on a 17-in. color monitor (FlexScan T562-T, Eizo, Japan). Twelve-bit resolution was selected for each gun (compare with Ref. 21), and screen resolution was  $1024 \times 768$  pixels with a frame rate of 100 Hz. Calculation of the chromaticities and the luminances required for each stimulus was performed before the experiment. The monitor was switched on at least 30 min before each experimental session to allow its output to stabilize.

Before and at intervals during the experiment, the system was calibrated with a spectroradiometer (Spectra-Scan PR-650, Photo Research, Chatsworth, California), whose calibration was in turn traceable to a calibration by the UK National Physical Laboratory. Control measurements were performed to verify that the expected values of the chromaticities and the luminances coincided with the values produced in the experiment.<sup>26</sup>

#### 2. Stimuli

Stimuli were computer-generated images of illuminated Mondrian patterns (any subsequent reference to surfaces and illuminants used in the experiment applies to these computer simulations). The patterns were square, of side  $6^\circ$ , and consisted of  $49 (7 \times 7)$  square, colored surfaces of side  $0.86^\circ$ . The patterns were presented in a dark surround at a viewing distance of 50 cm. At this distance only a small area at the center of the screen needed to be used, allowing the stimuli to be displayed with a spatial variation of less than 0.005 in CIE 1931  $(x, y)$  coordinates and less than 1% in luminance. The surfaces making up the patterns were Munsell surfaces, whose spectral reflectances were generated from eight basis functions taken from a principal-components analysis<sup>27</sup> of 1257 samples from the Munsell Book of Color.<sup>28</sup> This set of basis functions reproduced accurately the spectral reflectances of a large set of natural surfaces such as flowers, flower clusters, leaves, and berries.<sup>29</sup> The illuminants were different phases of natural daylight, whose spectral power distributions were generated from three basis functions taken from a principal-

components analysis<sup>30</sup> of 622 samples of skylight and sunlight with skylight. Basis functions were used for computational efficiency rather than for any theoretical rationale connected with assumptions about the dimensionality of color-constancy models.<sup>31–36</sup>

Because the locus of natural daylights can be described by a contour in CIE 1931  $(x, y)$  color space,<sup>37</sup> the phase of each daylight can be conveniently represented by its  $x$  coordinate. Each Mondrian pattern was uniformly illuminated by a phase of daylight with initial  $x$  coordinate  $x_0$  either 0.25 or 0.37 (corresponding to a correlated color temperature of 25,000 or 4300 K).

The selected Mondrian patterns were subjected to two types of changes: illuminant-derived and nonilluminant-derived. For an illuminant-derived change, the  $x$  coordinate of the illuminant was incremented, uniformly over the image, by a constant value  $\Delta x$  of 0.03, 0.06, or 0.09 if the initial value  $x_0$  was 0.25, or by  $-0.03$ ,  $-0.06$ , or  $-0.09$  if the initial value  $x_0$  was 0.37. Six illuminant-change conditions were therefore possible. For a nonilluminant-derived change, the  $x$  coordinate of the illuminant was incremented spatially uniformly, exactly as for an illuminant-derived change, but an additional spatially nonuniform change was made: For a random selection of half of the surfaces, the  $x$  coordinate of the illuminant on each of those surfaces was incremented by a constant value  $\Delta x'$  equal to 0.01, 0.02, or 0.03; and, for the other half of the surfaces, it was incremented by a constant value  $\Delta x'$  equal to  $-0.01$ ,  $-0.02$ , or  $-0.03$ . (These non-uniform changes would be unlikely to correspond to any natural illuminant change; on grounds of parsimony, therefore, they should be attributed by observers to a change in the spectral-reflectance properties of the surfaces comprising the pattern.<sup>18,19,21</sup>) It is emphasized that these manipulations of the  $x$  coordinate referred to the phase of the illuminant only; the effect on the chromaticity coordinates of any particular patch in the image depended of course on the product of the illuminant and the reflectance spectra concerned. A total of 18 (6 illuminant-derived  $\times$  3 nonilluminant-derived) conditions were therefore tested for each type of image.

For unmodified images, a set of Munsell surfaces was chosen randomly and subjected to illuminant-derived and nonilluminant-derived changes also chosen randomly from the set of values just described. The luminances  $Y$  of the patches in each image, determined by the illuminant–reflectance products, fell generally in the range  $1.0\text{--}10.0 \text{ cd m}^{-2}$  with mean of approximately  $4.0 \text{ cd m}^{-2}$ . For achromatic images, copies of the unmodified images were prepared, and the  $(x, y)$  chromaticity coordinates of every patch were changed to (0.313, 0.329), the color of CIE Standard Illuminant  $D_{65}$ . For isoluminant images, copies of the unmodified images were prepared, and the luminance  $Y$  of every patch was adjusted so that it was  $4.0 \text{ cd m}^{-2}$ . These  $(x, y, Y)$  specifications of the images refer to the CIE 1931 standard observer; as to how well sensation-luminance cues<sup>38</sup> were actually suppressed in the isoluminant images is considered in Sections 3 and 4. Note that these isoluminant and achromatic images no longer correspond to simulations of illuminant and surfaces in the same way that the unmodified images do. Although very particular sets of sur-

faces and illuminants could in principle produce the specified chromaticities of the modified patterns, they would represent implausible natural events.

### 3. Design and Procedure

The two intervals of each trial in the forced-choice design were constructed as follows (compare with Ref. 18): In one interval of the trial, two successively presented Mondrian patterns were related by an illuminant-derived change; in the other interval of the trial, the two patterns were related by a nonilluminant-derived change, as explained in Subsection 2.A.2. Each image was presented for 1 s, and the delay between the two 2-s intervals was 1 s; each stimulus sequence therefore lasted 5 s. The observer's task was to identify which of the two changes in the Mondrian patterns appeared more like an illuminant change. Observers initiated each trial and made their responses on a push-button switch box connected to the computer. No feedback was given. Images were viewed in a darkened room.

In each trial the surfaces making up the Mondrian pattern were selected at random, as were the initial illuminant  $x_0$  and the illuminant-derived and nonilluminant-derived changes  $\Delta x$  and  $\Delta x'$ . In total, 180 trials were performed in each experimental session, which lasted approximately 1 h. Only one of the three types of images (unmodified, achromatic, or isoluminant) was used in each experimental session. The different image types were tested in cyclic order across sessions.

### 4. Observers

There were three observers, PA, AS, and PG, aged 22–25 yr. All had normal color vision, as assessed with the Farnsworth–Munsell 100-hue test and Ishihara plates, and normal visual (Snellen) acuity. All were unaware of the purpose of the experiment.

### B. Results and Comment

Figure 1 shows overall performance with the unmodified, achromatic, and isoluminant images averaged across all observers and illuminant variations. The percentage of illuminant-change responses to an illuminant-derived change was not reliably different over the three image types ( $p > 0.5$ ).

The graphs in Figs. 2 and 3 show in detail how performance varied with the size of the illuminant-derived and nonilluminant-derived changes. The percentage of illuminant-change responses is plotted against the nonuniform shift  $\Delta x'$  in illuminant CIE  $x$  value. The rows of graphs correspond to the kinds of images: unmodified, achromatic, and isoluminant. In Fig. 2 the columns of graphs correspond to different levels of uniform positive  $x$  shifts  $\Delta x$  of 0.03, 0.06, and 0.09 with an initial illuminant CIE  $x$  value  $x_0$  of 0.25. In Fig. 3 the columns of graphs correspond to different levels of uniform negative  $x$  shifts  $\Delta x$  of  $-0.03$ ,  $-0.06$ , and  $-0.09$  with an initial illuminant CIE  $x$  value  $x_0$  of 0.37. The different symbols are for different observers, each value being based on 50 trials. The lines through the data points are the results of model predictions, explained in Section 3.

There was a similar increase in the percentage of illuminant-change responses with an increase in the non-

uniform shift  $\Delta x'$  over the different image types and levels of illuminant change. Performance was well above chance levels for values of  $\Delta x'$  greater than 0.01. In some conditions it was close to 100%.

In summary, observers were able to make reliable discriminations of illuminant-derived changes from nonilluminant-derived changes with all three image types, implying that relational color constancy is not based on processing within either luminance or chromaticity pathways alone.

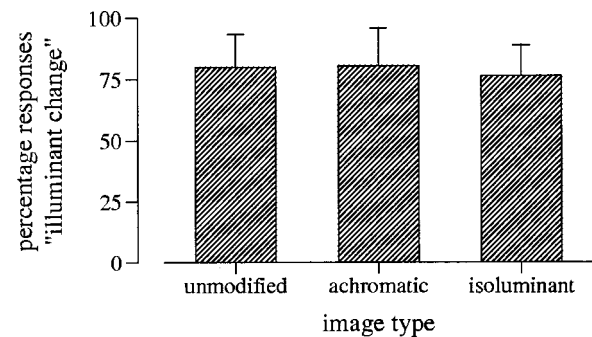


Fig. 1. Overall performance with the unmodified, achromatic, and isoluminant images averaged across all observers and illuminant variations. The percentage of illuminant-change responses to an illuminant-derived change is plotted against image type.

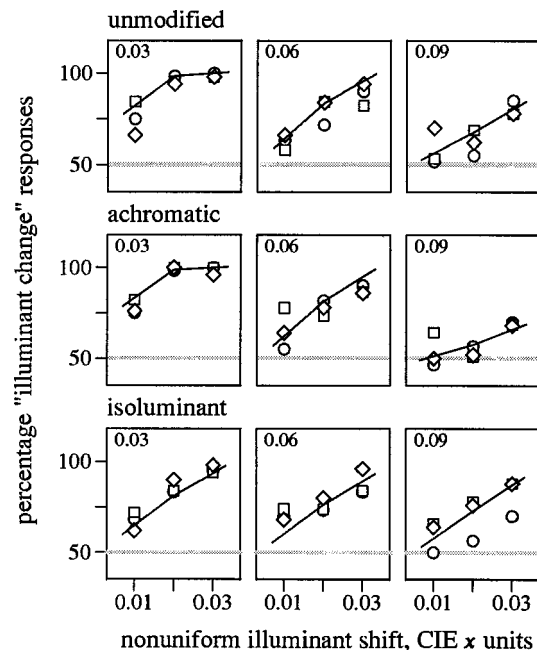


Fig. 2. Discriminability of illuminant-derived and non-illuminant-derived changes in images of Mondrian patterns as a function of nonuniform shift  $\Delta x'$  in illuminant CIE  $x$  value. The columns of the graphs correspond to different levels of uniform positive  $x$  shifts  $\Delta x$  of 0.03, 0.06, and 0.09 in illuminant CIE  $x$  value, and the rows of the graphs correspond to the kinds of images: unmodified, achromatic, and isoluminant. The initial illuminant CIE  $x$  value  $x_0$  was 0.25. The different symbols indicate different observers [circles (PA), squares (PG), and diamonds (AS)]. Each value was based on 50 trials. The lines through the data points are the results of model predictions based on ratios of cone excitations.



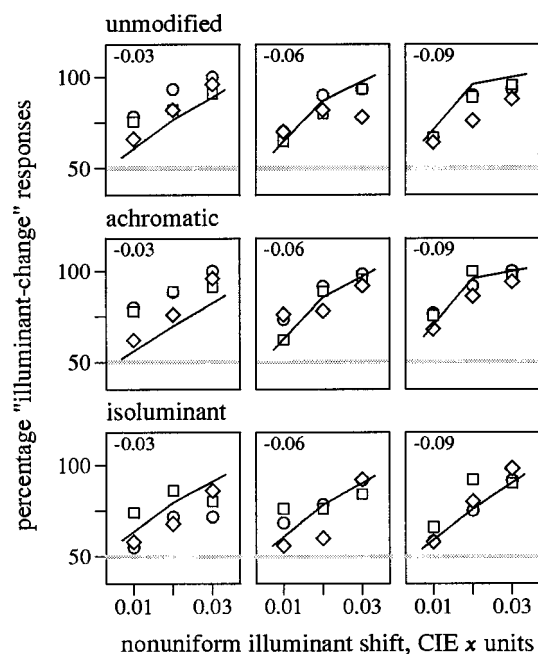


Fig. 3. Discriminability of illuminant-derived and non-illuminant-derived changes in images of Mondrian patterns as a function of nonuniform shift  $\Delta x'$  in illuminant CIE  $x$  value. The columns of the graphs correspond to different levels of uniform negative  $x$  shifts  $\Delta x$  of  $-0.03$ ,  $-0.06$ , and  $-0.09$  in illuminant CIE  $x$  value, and the rows of the graphs correspond to the kinds of images: unmodified, achromatic, and isoluminant. The initial illuminant CIE  $x$  value  $x_0$  was 0.37. Other details are the same as those for Fig. 2.

### 3. PREDICTIONS FROM PHYSICAL SIGNALS

#### A. Invariant Ratios of Cone Excitations and of Combinations of Cone Excitations

Does the coding of color relations described in Section 1 offer an adequate basis for predicting the detailed discrimination performance shown in Figs. 2 and 3? Although spatial ratios of cone excitations are generally invariant under surface illuminant changes, are they invariant for the modified images tested here? And does this invariance extend to postreceptoral, nonopponent and opponent, combinations of cone excitations? To address these questions, a computational analysis was performed as follows. Exactly as in the psychophysical experiments, illuminants were taken from the different phases of natural daylight, with CIE  $x$  values ranging from 0.25 to 0.37, and surfaces from the Munsell Book of Color. All spectral distributions were defined over the range 400–700 nm at 10-nm intervals, the interval available for the daylight spectra. Cone excitations were determined from the CIE  $(x, y)$  chromaticity coordinates and the luminance  $Y$  of each colored patch. The Smith and Pokorny<sup>39,40</sup> set of cone fundamentals was used; chromaticity coordinates were first converted to the Judd-modified  $(x', y')$  values and then to cone excitations. Ratios of cone excitations and ratios of combinations of cone excitations produced by pairs of surfaces were determined for 1000 randomly chosen samples of pairs of illuminants and pairs of surfaces (see Ref. 20). Details of these combinations are given below. These computations were per-

formed for each of the colorimetrically unmodified, achromatic, and isoluminant images tested psychophysically.

The departure from invariance of these ratios was quantified by the relative deviation, as follows. In any iteration of the simulation, let  $r_1$  and  $r_2$  be the (nonzero) ratios of cone excitations in a particular cone class that are due to light reflected from a pair of surfaces under illuminants 1 and 2, respectively. One possible definition of the relative deviation is  $|r_1 - r_2|/(r_1 + r_2)$ , which, as a measure, has the form of a (Michelson) contrast and is zero for strictly invariant ratios. For consistency with previous reports,<sup>20,21</sup> however, the more sensitive measure given by  $|r_1 - r_2|/\min(r_1, r_2)$  was used. (In fact, for the average deviations reported here, the two measures differed by a constant scale factor of almost exactly 2.0.) The first three columns of numbers in Table 1, labeled  $r$ ,  $g$ , and  $b$ , show the results of the simulations, expressed as relative deviations for long-, medium-, and short-wavelength-sensitive cones, respectively, averaged over the 1000 combinations of illuminant and surfaces. For all three types of images, the average relative deviation was small, in all conditions not more than 0.033.

The average relative deviation was slightly greater with achromatic images than with colorimetrically unmodified images and was smaller with isoluminant images, except for short-wavelength-sensitive cones. The average relative deviation with achromatic images was of course the same for each cone class, as each was excited in constant proportion to the other.

Combinations of cone excitations yielded similar results. Three combinations were considered: a simple (positively weighted) sum of cone excitations, representing a possible nonopponent luminance signal  $L$  (equal to the CIE  $Y$  value); and two differences of cone excitations, representing possible opponent-color signals, namely, a "red-green" signal  $r - g$  formed from the difference in excitations of long- and medium-wavelength-sensitive cones, and a "blue-yellow" signal  $b - y$  formed from the difference in excitations of short-wavelength-sensitive cones and the sum of excitations of long- and medium-wavelength-sensitive cones (the weights reflecting the Wyszecki and Stiles tabulation<sup>37</sup>). These particular combinations of excitations were chosen for illustrative purposes only; other combinations of cone excitations, drawn from a range of opponent-color models, are considered in Subsection 3.B. The specific combinations of cone excitations considered here should be distinguished from less constrained combinations used in some computational analyses of color constancy (e.g., Refs. 41 and 42; see also

**Table 1. Relative Deviations in Spatial Ratios of Excitations for Each Cone Class and for Luminance and Opponent-Color Combinations of Cone Excitations**

Image	Cones			Cone Combinations		
	$r$	$g$	$b$	$L$	$r - g$	$b - y$
Unmodified	0.028	0.024	0.013	0.033	0.018	0.027
Achromatic	0.029	0.029	0.029	0.033	0.033	0.033
Isoluminant	0.003	0.009	0.033	0	0.017	0.001

Ref. 43), which, nevertheless, have yielded psychophysically plausible results.

Thus ratios of these combinations of cone excitations produced by pairs of surfaces were determined, as for ratios of cone excitations, for 1000 randomly chosen samples of pairs of illuminants and pairs of surfaces and for each of the three types of images: colorimetrically unmodified, achromatic, and isoluminant. (Although it was assumed that with achromatic images only the short-, medium-, and long-wavelength-sensitive cones were excited in constant proportion to each other, it was not assumed that the signals  $r - g$  and  $b - y$  were necessarily zero; but see Subsection 3.B). The last three columns of Table 1, labeled  $L$ ,  $r - g$ , and  $b - y$ , show the results of the simulations expressed as relative deviations, for luminance and the two opponent-color signals, respectively, averaged across the 1000 combinations of illuminant and surfaces. For all three types of images, the average relative deviation was again small, in all conditions not more than 0.033. With achromatic images the relative deviation was approximately the same as or slightly larger than that with the unmodified images, and with isoluminant images it was smaller. Fractional combinations of cone excitations were also tested; for example, a red-green signal as  $r - kg$ , where  $0 < k < 1$ , which yielded slightly smaller relative deviations in some conditions.

## B. Predictions of Performance

Suppose that observers did indeed use ratios of cone excitations or of combinations of cone excitations to decide in each trial whether there was an illuminant or nonilluminant change. Was discrimination performance then accurately predicted? A computational simulation was performed in which the cue for discrimination was assumed to be based on relative deviations in ratios of cone excitations or on relative deviations in ratios of nonopponent and opponent combinations of cone excitations. In each trial two signals were assumed to be generated:  $s_1$ , a relative-deviation signal for a pair of Mondrian patterns undergoing an illuminant-derived change, and  $s_2$ , a relative-deviation signal for a pair of Mondrian patterns undergoing a nonilluminant-derived change. The ratios of cone excitations or combinations of cone excitations were estimated from the color coordinates of the simulated surfaces and illuminant used in each trial of the experiment. Relative deviations for pairs of adjacent surfaces, defined as in Subsection 3.A, were averaged over all pairs in the image. The signals  $s_1$  and  $s_2$  were actually defined as weighted sums, with coefficients  $\alpha$ ,  $\beta$ , and  $\gamma$ , of the three averaged relative deviations for the three kinds of cone excitations (long-, medium-, and short-wavelength-sensitive) and for the three kinds of combinations of cone excitations ( $L$ ,  $r - g$ , and  $b - y$ ).

Observers were assumed to compare  $s_1$  with  $s_2$ . The difference  $s_1 - s_2$  was treated as a random variable. Thus, if  $\Phi$  is the cumulative unit normal distribution and  $\sigma$  is the spread of the response function, which, for simplicity, was assumed to be the same for all stimuli and conditions, the probability of an illuminant-change response being generated is  $\Phi((s_1 - s_2)/\sigma)$ . Performance was estimated for all 18 conditions of the experiment (yielding 54 data points), and the results were compared

**Table 2. Root Mean Square Error (RMSE) for Fits of Models Based on Relative Deviations in Ratios of Cone Excitations and in Ratios of Nonopponent and Opponent Combinations of Cone Excitations**

	$r, g, b$	$L, r - g, b - y$	DKL <sup>a</sup>	DD <sup>b</sup>
RMSE of fits (%)	6.4	8.9	9.1	10.8

<sup>a</sup>Three-dimensional space described by Derrington *et al.*<sup>45</sup>

<sup>b</sup>Anatomically oriented multistage model described by De Valois and De Valois.<sup>46</sup>

with the experimental data averaged across observers. The values of  $\sigma$  and the weights  $\alpha$ ,  $\beta$ , and  $\gamma$  were optimized by Brent's method<sup>44</sup> to produce the best fit to the observed data.

Results for fits based on ratios of cone excitations are shown in Figs. 2 and 3 by the solid lines. (The corresponding values of the weights  $\alpha$ ,  $\beta$ , and  $\gamma$  were such that the contributions of the long- and medium-wavelength-sensitive cones were similar and the contribution of the short-wavelength-sensitive cones was small.) The model accounted adequately for the variance in the data [root mean square error (RMSE) of 6.4%, compared with a within-observer standard deviation also of 6.4%]. The fits based on ratios of opponent and nonopponent combinations of cone excitations were slightly poorer (RMSE of 8.9%).

For achromatic and unmodified images, predictions based solely on luminance signals were close to the experimental data, but, because in the isoluminant condition luminance ratios were invariant for both illuminant and spectral-reflectance changes, predicted levels were here 50%. A luminance signal cannot, therefore, provide a plausible cue in this condition. In an attempt to account for individual variations in the luminous efficiency function,<sup>38</sup> the relative contributions of the long- and medium-wavelength-sensitive cone excitations were allowed to vary for individual observers, and the predictions were reevaluated. The resulting fits based solely on luminance signals remained poor.

Other combinations of cone excitations were also considered: one based on the three-dimensional space described by Derrington *et al.*<sup>45</sup> in which opponent combinations produce zero response for the achromatic images (cf. the opponent combinations considered in Subsection 3.A), and another based on the anatomically oriented multistage model described by De Valois and De Valois,<sup>46</sup> in which at a cortical stage red-green and blue-yellow axes are separated and luminance is separated from color. The goodness of fits for ratios of these various combinations of cone signals are given in Table 2. None provided better fits than those with ratios of cone excitations.

## 4. DISCUSSION

Discrimination between Mondrian patterns undergoing illuminant-derived and nonilluminant-derived changes was possible with isoluminant images, for which there were no luminance cues, and with achromatic images, for which there were no chromaticity cues. It might be argued that because luminance values in the isoluminant

images were defined with respect to the CIE 1931 standard observer, individual differences in sensation luminance<sup>38</sup> might have been sufficient to generate useful residual luminance cues for discrimination performance. But this seems unlikely, as such cues would certainly have been smaller with the nominally isoluminant images than with unmodified images, whereas the corresponding performance levels were broadly similar. Moreover, as was indicated in Subsection 3.B, allowing for individual variations in the luminous efficiency function did not improve fits to the data.

The computational simulations of cone activity summarized in Table 1 showed that whether the images were isoluminant, achromatic, or colorimetrically unmodified, spatial ratios of excitations produced in a given class of cones by light reflected from pairs of surfaces were almost invariant under changes in illuminant. This level of invariance was preserved when ratios of sums of cone excitations, that is, ratios of luminance signals, and ratios of differences of cone excitations, that is, ratios of opponent-color signals, were computed.

It is not unreasonable that spatial ratios of sums of cone excitations should yield levels of invariance that are approximately as good as spatial ratios of cone excitations. This result may be partly attributable to the large correlation between cone excitations for long- and medium-wavelength-sensitive cones.<sup>47–50</sup> Difference signals can produce spectral sensitivities that are sharper than those of cones alone<sup>51,52</sup>; and ratios of these spectrally sharpened signals are even more stable under illuminant changes than cone-excitation ratios. The latter effect may be seen for colorimetrically unmodified images in the smaller mean percentage relative variation in  $r - g$  ratios (Table 1) than in either long- or medium-wavelength-sensitive-cone-excitation ratios alone. The same level of sharpening does not occur with  $b - y$  ratios (as there is less overlap of spectral sensitivities); their mean percentage relative variation was greater than that with ratios of short-wavelength-sensitive-cone excitations alone.

The close correspondence between data and predictions shown in Figs. 2 and 3 supports the notion that the discrimination of illuminant changes from nonilluminant changes—and by implication relational color constancy—might be mediated by spatial ratios of cone excitations. The small relative contribution of the short-wavelength-sensitive cones to discrimination performance is consistent with the findings of previous experiments.<sup>21</sup> Models with the same number of adjustable parameters but based on ratios of combinations of cone excitations were able to predict the general trends of the data but described its detailed features less well. Even so, given the simplicity of the model (e.g., no allowance was made for variations in the perceptual salience of deviations in ratios of cone excitations across the image), it would be unwise to exclude the possibility of ratios of combinations of cone excitations mediating discrimination performance.

In conclusion, discriminations underlying relational color constancy seem not to depend on either luminance or chromaticity cues alone, at least with the kinds of images tested here. Discrimination could be based on a visual coding of spatial color relations, but these relations

would need to be defined for both achromatic and isoluminant images. Such a coding could be provided by spatial ratios of cone excitations or of nonopponent and opponent combinations of cone excitations computed at some more central visual locus.

## ACKNOWLEDGMENTS

This work was supported by the Wellcome Trust (grant 034807), the Biotechnology and Biological Sciences Research Council (grant S08656), the Centro de Física da Universidade do Minho, Braga, Portugal, and the British Council. We thank L. M. Doherty, K. J. Linnell, and C. J. Savage for critical reading of the manuscript, D. H. Brainard, M. D'Zmura, and an anonymous reviewer for helpful suggestions, and J. P. S. Parkkinen, J. Hallikainen, and T. Jaaskelainen for providing data for the spectral reflectances of the Munsell papers.

Address correspondence to Sérgio M. C. Nascimento at the Universidade do Minho location on the title page or by e-mail, smcn@fisica.uminho.pt.

## REFERENCES

1. T. Young, *A Course of Lectures on Natural Philosophy and the Mechanical Arts* (Joseph Johnson, London, 1807), Vol. I, Lecture XXXVIII.
2. H. von Helmholtz, *Handbuch der Physiologischen Optik*, 1st ed. (Leopold Voss, Leipzig, 1867), Vol. II; *Helmholtz's Treatise on Physiological Optics*, translation of 3rd ed., J. P. C. Southall, ed. (Optical Society of America, Washington, D.C., 1924), pp. 286–287 (republished by Dover, New York, 1962).
3. E. H. Land, "Color vision and the natural image. Part I," *Proc. Natl. Acad. Sci. USA* **45**, 115–129 (1959).
4. E. H. Land, "Color vision and the natural image. Part II," *Proc. Natl. Acad. Sci. USA* **45**, 636–644 (1959).
5. E. H. Land and J. J. McCann, "Lightness and Retinex theory," *J. Opt. Soc. Am.* **61**, 1–11 (1971).
6. L. Arend and A. Reeves, "Simultaneous color constancy," *J. Opt. Soc. Am. A* **3**, 1743–1751 (1986).
7. L. Arend, A. Reeves, J. Schirillo, and R. Goldstein, "Simultaneous color constancy: papers with diverse Munsell values," *J. Opt. Soc. Am. A* **8**, 661–672 (1991).
8. D. I. Bramwell and A. C. Hurlbert, "The role of object recognition in colour constancy," *Perception* **22**, 62–63 (1993).
9. D. I. Bramwell and A. C. Hurlbert, "Measurements of colour constancy using a forced-choice matching technique," *Perception* **25**, 229–241 (1996).
10. M. P. Lucassen and J. Walraven, "Quantifying color constancy: evidence for nonlinear processing of cone-specific contrast," *Vision Res.* **33**, 739–757 (1993).
11. M. P. Lucassen and J. Walraven, "Color constancy under natural and artificial illumination," *Vision Res.* **36**, 2699–2711 (1996).
12. F. W. Cornelissen and E. Brenner, "Simultaneous colour constancy revisited: an analysis of viewing strategies," *Vision Res.* **35**, 2431–2448 (1995).
13. D. H. Brainard, W. A. Brunt, and J. M. Speigle, "Color constancy in the nearly natural image. I. Asymmetric matches," *J. Opt. Soc. Am. A* **14**, 2091–2110 (1997).
14. K. Bäuml, "Illuminant changes under different surface collections: examining some principles of color appearance," *J. Opt. Soc. Am. A* **12**, 261–271 (1995).
15. K. Bäuml, "Simultaneous color constancy: how surface color perception varies with the illuminant," *Vision Res.* **39**, 1531–1550 (1999).
16. K. Bäuml, "Color constancy: the role of image surfaces in



- illuminant adjustment," J. Opt. Soc. Am. A **16**, 1521–1530 (1999).
17. J. M. Kraft and D. H. Brainard, "Mechanisms of color constancy under nearly natural viewing," Proc. Natl. Acad. Sci. **96**, 307–312 (1999).
  18. B. J. Craven and D. H. Foster, "An operational approach to colour constancy," Vision Res. **32**, 1359–1366 (1992).
  19. D. H. Foster, B. J. Craven, and E. R. H. Sale, "Immediate colour constancy," Ophthalmic Physiol. Opt. **12**, 157–160 (1992).
  20. D. H. Foster and S. M. C. Nascimento, "Relational colour constancy from invariant cone-excitation ratios," Proc. R. Soc. London, Ser. B **257**, 115–121 (1994).
  21. S. M. C. Nascimento and D. Foster, "Detecting natural changes of cone-excitation ratios in simple and complex coloured images," Proc. R. Soc. Lond, Ser. B **264**, 1395–1402 (1997).
  22. A. L. Gilchrist and A. Jacobsen, "Lightness constancy through a veiling luminance," J. Exp. Psychol.: Hum. Percept. Perform. **9**, 936–944 (1983).
  23. L. E. Arend and R. Goldstein, "Simultaneous constancy, lightness and brightness," J. Opt. Soc. Am. A **4**, 2281–2285 (1987).
  24. L. E. Arend and B. Spehar, "Lightness, brightness, and brightness contrast: 1. Illuminance variation," Percept. Psychophys. **54**, 446–456 (1993).
  25. M. D'Zmura and A. Mangalick, "Detection of contrary chromatic change," J. Opt. Soc. Am. A **11**, 543–546 (1994).
  26. R. S. Berns, M. E. Gorzynski, and R. J. Motta, "CRT colorimetry. Part II: Metrology," Color Res. Appl. **18**, 315–325 (1993).
  27. J. P. S. Parkkinen, J. Hallikainen, and T. Jaaskelainen, "Characteristic spectra of Munsell colors," J. Opt. Soc. Am. A **6**, 318–322 (1989).
  28. *Munsell Book of Color—Matte Finish Collection* (Munsell Color Corp., Baltimore, Md., 1976).
  29. T. Jaaskelainen, J. Parkkinen, and S. Toyooka, "Vector-subspace model for color representation," J. Opt. Soc. Am. A **7**, 725–730 (1990).
  30. D. B. Judd, D. L. MacAdam, and G. Wyszecki, "Spectral distribution of typical daylight as a function of correlated color temperature," J. Opt. Soc. Am. **54**, 1031–1040 (1964).
  31. L. T. Maloney and B. A. Wandell, "Color constancy: a method for recovering surface spectral reflectance," J. Opt. Soc. Am. A **3**, 29–33 (1986).
  32. L. T. Maloney, "Evaluation of linear models of surface spectral reflectance with small numbers of parameters," J. Opt. Soc. Am. A **3**, 1673–1683 (1986).
  33. L. T. Maloney, "Color constancy and color perception: the linear-models framework," in *Attention and Performance XIV*, D. E. Meyer and S. Kornblum, eds. (MIT Press, Cambridge, Mass., 1993), pp. 59–78.
  34. M. D'Zmura and G. Iverson, "Color constancy. I. Basic theory of two-stage linear recovery of spectral descriptions for lights and surfaces," J. Opt. Soc. Am. A **10**, 2148–2165 (1993).
  35. M. D'Zmura and G. Iverson, "Color constancy. II. Results for two-stage linear recovery of spectral descriptions for lights and surfaces," J. Opt. Soc. Am. A **10**, 2166–2180 (1993).
  36. M. D'Zmura and G. Iverson, "Color constancy. III. General linear recovery of spectral descriptions for lights and surfaces," J. Opt. Soc. Am. A **11**, 2389–2400 (1994).
  37. G. Wyszecki and W. S. Stiles, *Color Science: Concepts and Methods, Quantitative Data and Formulae* (Wiley, New York, 1982).
  38. P. K. Kaiser, "Sensation luminance: a new name to distinguish CIE luminance from luminance dependent on an individual's spectral sensitivity," Vision Res. **28**, 455–456 (1988).
  39. V. C. Smith and J. Pokorny, "Spectral sensitivity of color-blind observers and the cone photopigments," Vision Res. **12**, 2059–2071 (1972).
  40. V. C. Smith and J. Pokorny, "Spectral sensitivity of the foveal cone photopigments between 400 and 500 nm," Vision Res. **15**, 161–171 (1975).
  41. G. D. Finlayson, M. S. Drew, and B. V. Funt, "Spectral sharpening: sensor transformations for improved color constancy," J. Opt. Soc. Am. A **11**, 1553–1563 (1994).
  42. G. D. Finlayson, M. S. Drew, and B. V. Funt, "Color constancy: generalized diagonal transforms suffice," J. Opt. Soc. Am. A **11**, 3011–3019 (1994).
  43. Q. Zaidi and A. G. Shapiro, "Adaptive orthogonalization of opponent-color signals," Biol. Cybern. **69**, 415–428 (1993).
  44. R. P. Brent, *Algorithms for Minimization without Derivatives* (Prentice-Hall, Englewood Cliffs, N.J., 1973).
  45. A. M. Derrington, J. Krauskopf, and P. Lennie, "Chromatic mechanisms in lateral geniculate nucleus of Macaque," J. Physiol. (London) **357**, 241–265 (1984).
  46. R. L. De Valois and K. K. De Valois, "A multi-stage color model," Vision Res. **33**, 1053–1065 (1993).
  47. G. Buchsbaum and A. Gottschalk, "Trichromacy, opponent colours coding and optimum colour information transmission in the retina," Proc. R. Soc. London, Ser. B **220**, 89–113 (1983).
  48. Q. Zaidi, B. Spehar, and J. DeBonet, "Color constancy in variegated scenes: role of low-level mechanisms in discounting illumination changes," J. Opt. Soc. Am. A **14**, 2608–2621 (1997).
  49. Q. Zaidi, "Decorrelation of L- and M-cone signals," J. Opt. Soc. Am. A **14**, 3430–3431 (1997).
  50. Q. Zaidi, "Identification of illuminant and object colors: heuristic-based algorithms," J. Opt. Soc. Am. A **15**, 1767–1776 (1998).
  51. H. G. Sperling and R. S. Harwerth, "Red-green cone interactions in the increment-threshold spectral sensitivity of primates," Science **172**, 180–184 (1971).
  52. D. H. Foster and R. S. Snelgar, "Test and field spectral sensitivities of colour mechanisms obtained on small white backgrounds: action of unitary opponent-colour processes?" Vision Res. **23**, 787–797 (1983).